Supplementary Information

Factors maximising photoinduced electron-transfer-coupled phase migration to boost biphasic photocatalysis

Ren Itagaki,[a] Akinobu Nakada,[a] Hajime Suzuki,[a,b] Osamu Tomita,[a] Ryu Abe[a]**

[a] Department of Energy and Hydrocarbon Chemistry, Graduate School of Engineering, Kyoto University, Nishikyo-ku, Kyoto 615-8510, Japan.
[b] Precursory Research for Embryonic Science and Technology (PRESTO), Japan Science and Technology Agency (JST), 4-1-8 Honcho, Kawaguchi, Saitama 332-0012, Japan.

*E-mail: nakada@scl.kyoto-u.ac.jp (A.N.), ryu-abe@scl.kyoto-u.ac.jp (R.A.)
Phone: +81-75-383-7044. Fax: +81-75-383-2479.

General procedure

^{1}H NMR (400 MHz) spectra were measured on a JEOL ECX-400 spectrometer. UV-vis absorption and emission spectra were recorded at room temperature on Shimadzu U1800 and a JASCO Model FP-8550 spectrofluorometer, respectively. Emission lifetimes were measured on a Horiba DeltaFlex (excitation source: NanoLED-440L). Elemental analyses were carried out on a PerkinElmer 2400 II CHN analyser.

Synthesis and characterisation

$[Ir(C6)_2(dmb)]PF_6$ (**Ir**) was synthesized according to a slightly modified literature procedure.[1] An Ir(III) μ-chloro-bridged dimer complex, which was used as a precursor for the target complex **Ir** was synthesized as previously reported.[2] A suspension of the dimer complex (0.104 g, 0.056 mmol) and dmb (0.023 g, 0.125 mmol) in ethylene glycol (5.6 mL) was stirred for 2 h at 150 ºC under a nitrogen atmosphere. After cooling to room temperature, the reaction mixture was poured into water (40 mL) and NH_4PF_6 (0.407 g, 2.497 mmol in 4 mL of water) was added. The resulting precipitate was extracted into CH_2Cl_2 (2 × 50 mL), before the organic phase was separated, dried over $MgSO_4$, and filtered. After all volatiles had been removed from the filtrate under reduced pressure, the obtained crude product was purified by column chromatography on silica gel (methanol/CH_2Cl_2 = 5:95, *v*/*v*), followed by recrystallisation from CH_2Cl_2/*n*-hexane, which afforded **Ir** as red crystals (0.086 g, 0.068 mmol, 63% yield). ^{1}H NMR (400 MHz, acetone-d_6): δ 8.85 (d, J = 6.0 Hz, 2H), 8.53 (s, 2H), 8.08 (d, J = 8.5 Hz, 2H), 7.77 (d, J = 5.0 Hz, 2H), 7.31 (t, J = 7.2 Hz, 2H), 7.02 (t, J = 7.2 Hz, 2H), 6.42 (d, J = 3.5 Hz, 2H), 6.17 (d, J = 9.5 Hz, 2H), 6.10-6.07 (m, 4H), 3.40 (q, J = 7.7 Hz, 6H), 2.60 (s, 6H), 1.06 (t, J = 7.3 Hz, 12H). Anal. Calcd. for $C_{52}H_{46}F_6IrN_6O_4PS_2 \cdot 0.5CH_2Cl_2$: C, 49.91; H, 3.75; N, 6.65. Found: C, 49.80; H, 3.67; N, 6.59.

Ferrocenium hexafluorophosphate ($Fc^+PF_6^-$) was synthesized from Fc according to a previously reported procedure.[3] The yield was 91% (4.55 g). Anal. Calcd for $C_{10}H_{10}F_6PFe$: C, 36.29; H, 3.05; N, 0.00; found: C, 36.27; H, 2.79; N, 0.02. UV-vis absorption: λ_{max} = 618 nm (ε_{max} = 420 M^{-1} cm^{-1}). An aqueous solution of ferrocenium chloride (Fc^+Cl^-) was prepared by an ion-exchange method. $Fc^+PF_6^-$ was dissolved in an aqueous TBACl solution (1 equiv, pH 2.5 adjusted with HCl) under an Ar atmosphere to avoid decomposition by O_2.[4-6] The resulting blue suspension was filtered to remove precipitated $TBAPF_6$. UV-vis absorption: λ_{max} = 618 nm (ε_{max} = 420 M^{-1} cm^{-1}).

Emission-quenching measurements

Emission spectrum of **Ir** (0.25 μM) in an organic solution was measured upon excitation at λ = 480 nm in a septum-sealed Pyrex cell (10 mm × 10 mm) after sparging with Ar (> 99.999%) for 20 min in the absence or presence of Fc at various concentrations ([Fc]; 0–0.3 mM). The emission intensity decreased as the concentration of Fc was increased, indicating the occurrence of photoinduced electron transfer from Fc to excited **Ir**. The reductive quenching followed the Stern-Volmer equation[7] (Eq. S1).

$$I_0/I = k_q \tau_0 [Fc] + 1 \quad \text{(S1a)}$$

$$\eta_q = 100 \times (1 - 1/(1 + k_q \tau_0 [Fc])) \quad \text{(S1b)}$$

where I_0 and I are emission intensity at 590 nm in the absence and presence of quencher, respectively.

Electrochemical measurements

Cyclic voltammetry measurements were conducted on a BAS model 650A electrochemical analyser, using a glassy carbon working electrode (ϕ = 3 mm) and a platinum-wire counter electrode. The reference electrode was made of a silver wire, inserted into a small glass tube fitted with a porous Vycor frit at the tip, and filled with a MeCN solution containing 0.1 M $TBAPF_6$ and 0.01 M $AgNO_3$. Unless otherwise noted, 0.1 M $TBAPF_6$ was used as the supporting electrolyte; for MeCN/H_2O (1:1, *v*/*v*) mixed solutions, 0.1 M $TEABF_4$ was used instead due to its higher solubility in the mixed solvent. The cyclic voltammetry measurements were carried out at 298 K using Fc (0.5 mM) and electrolyte (0.1 M), with scan rates (v) of 50–200 mV s^{-1}.

The anodic peak current (I_p) of Fc increased linearly with the square root of the scan rate ($v^{1/2}$), and plots of I_p versus $v^{1/2}$ gave straight lines for each solvent. The diffusion coefficient (D) of Fc in each solvent was estimated from the slopes of the Randles–Sevcik plots using Eq. S2.

$$I_p = 0.4463n^{3/2}F^{3/2}A[\mathrm{Fc}](RT)^{-1/2}v^{1/2}D^{1/2} \quad \text{(S2)}$$

where n is the number of electrons, F is Faraday's constant, A is the working-electrode area, [Fc] is the concentration of Fc, R is the gas constant, and T is absolute temperature.

When D was plotted against the reciprocal viscosity (μ^{-1}) of the solvents, an approximately linear relationship was obtained. This dependence is consistent with the Stokes–Einstein equation (Eq. S3), suggesting that specific-solvation effects of Fc are minor and that the diffusion process is governed mainly by the bulk viscosity of the medium (Fig. S2f).

$$D = k_B T / (6\pi r\mu) \quad \text{(S3)}$$

where k_B is Boltzmann's constant, T is absolute temperature, and r is radius of molecule. These electrochemical data provide the diffusion coefficients of Fc in the organic solvents used in the biphasic photocatalytic experiments.

Photocatalytic reactions

A solution of Fc (5.0 mM), **Ir** (0.05 mM), and Bn-Br (50 mM) in an organic solution (1.0 mL) was placed in a test tube (inner diameter: 10 mm; volume: 8.4 mL), before water was added (1.0 mL). The partition coefficient of each component was estimated based on the absorption spectra before photoirradiation. The biphasic solution was degassed by Ar sparging (10 min) and irradiated at λ = 470 nm using an LED lamp (CL-H1-470-9-1, Asahi Spectra Co.) with vigorous stirring. The product of the aqueous phase, i.e., Fc^+ was analysed by UV-vis absorption spectra in a quartz cell (1 mm × 10 mm), while the organic phase, i.e., Bn_2, was analysed and quantified by high performance liquid chromatography (Fig. S5). HPLC analyses were performed using a Shimadzu LC-20AD system equipped with a Phenomenex column (250 × 4.6 mm, 4 μm). A MeCN/H_2O (80:20, *v*/*v*) solution was used as the eluent at a flow rate of 1.0 mL min^{-1} (column temperature: 313 K), and a Shimadzu SPD-10A was used as the UV-vis detector. Under these analytical conditions, the retention times were determined using purchased or as-prepared samples (Fig. S7).

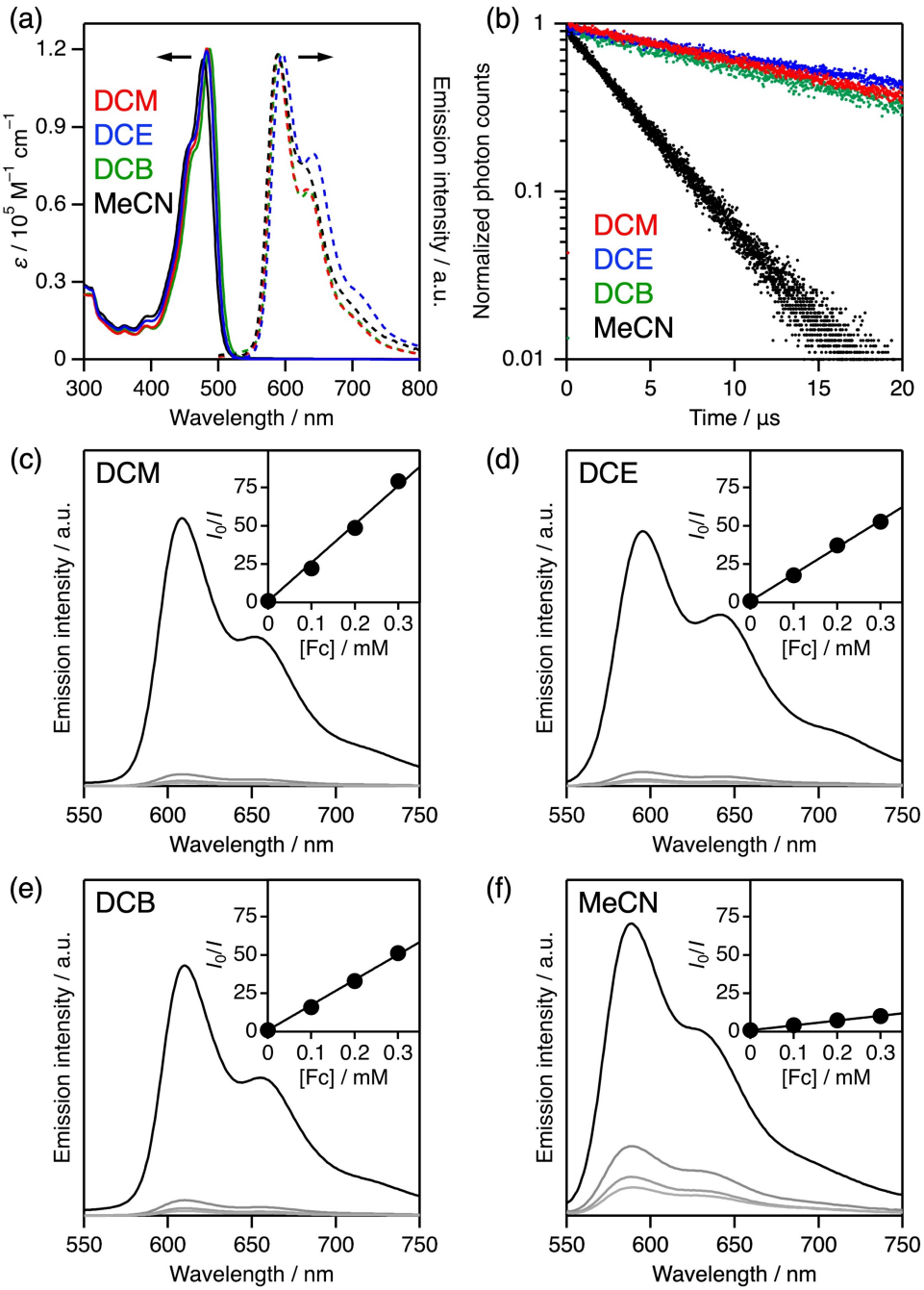

Fig. S1 (a) Steady-state UV-visible absorption and emission spectra (λ_{ex} = 480 nm), and (b) emission decay (λ_{ex} = 440 nm; λ_{em} = 590 nm) of **Ir** in DCM, DCE, DCB, and MeCN solutions. Emission spectra of **Ir** in the presence of various concentrations of Fc (0–0.3 mM) in (c) DCM, (d) DCE, (e) DCB, and (f) MeCN solutions. Inset: Stern-Volmer quenching of **Ir** by Fc.

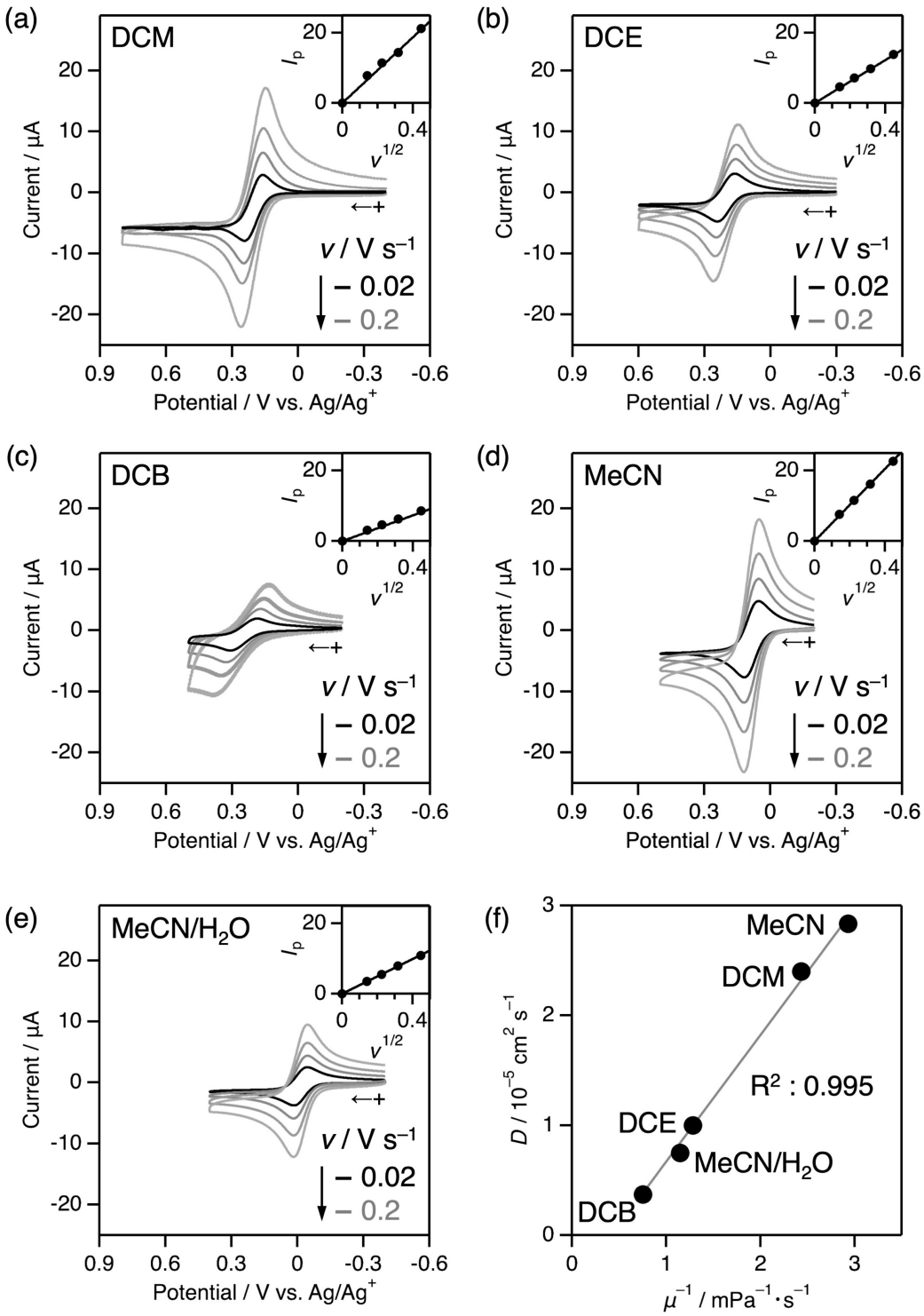

Fig. S2 Cyclic voltammograms of Fc in (a) DCM, (b) DCE, (c) DCB, (d) MeCN, and (e) MeCN/H_2O recorded at different scan rates. Inset: Randles–Sevcik plots. (f) Relationship between the diffusion coefficient (D) of Fc and the reciprocal viscosity (μ^{-1}) of the solvents.

Table S1 ^{1}H NMR integration data and calculated amounts/concentrations of organic solvents dissolved in the D_2O-rich phase after stirring[a]

Organic solvent	$[(NH_4)_2SO_4]$ in D_2O / M	δ_{Org} [b]	Integration (Number of H)[c]	Organic solvent dissolved in D_2O Amount / μmol[d]	Concentration / M[e]
DCM	0	5.44	10.69 (2H)	32.1	0.06
DCM	2.0	5.44	1.98 (2H)	5.94	0.01
DCE	0	3.83	6.49 (4H)	9.74	0.02
DCE	2.0	3.83	1.42 (4H)	2.13	0.004
DCB	0	7.55, 7.30	0.10[f] (4H)	0.2	0.0003
DCB	2.0	N.D.[g]	N.D.[g]	0	0
MeCN	0	2.06	1070 (3H)	2140	3.96
MeCN	0.5	2.06	492.86 (3H)	985.7	1.83
MeCN	1.0	2.06	373.95 (3H)	747.9	1.39
MeCN	1.5	2.06	263.75 (3H)	527.5	0.98
MeCN	2.0	2.06	152.85 (3H)	305.7	0.57

[a] Standard conditions: A biphasic solution containing organic solvent and D_2O (2 mL; 1:1, *v*/*v*) in the absence or presence of various concentrations of $(NH_4)_2SO_4$ (0.5–2.0 M) was vigorously stirred overnight. For quantitative ^{1}H NMR measurements, 540 μL of the D_2O-rich phase was collected, 60 μL of 0.1 M 4,4-dimethyl-4-silapentane-1-sulfonic acid (DSS) D_2O-solution was added as a standard (see Fig. S3). [b] Chemical shift(s) of the organic solvent. [c] Integration values of the organic-solvent signals (with the indicated number of protons) normalized to DSS (6 μmol). [d] (6 μmol) × (Integration) / (Number of H). [e] Concentration was calculated based on the sampled D_2O-rich phase volume (540 μL) prior to DSS addition. [f] Sum of signals. [g] N.D. = not detected.

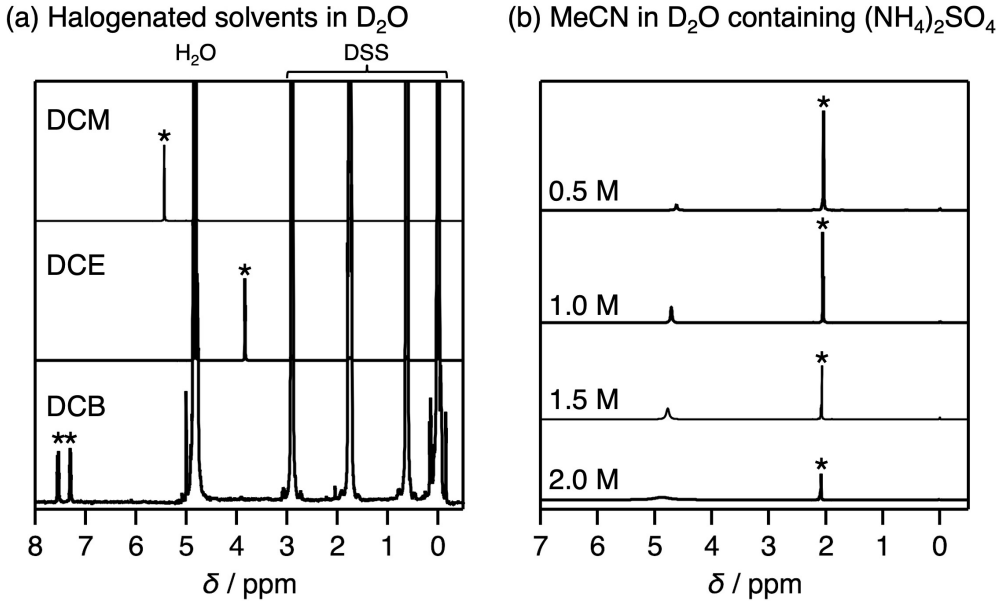

Fig. S3 ^{1}H NMR spectra of D_2O-rich phase: A biphasic solution containing organic solvent (a) halogenated solvents and (b) MeCN, and D_2O (2 mL; 1:1, *v*/*v*) in the absence or presence of various concentrations of $(NH_4)_2SO_4$ (0.5–2.0 M) was vigorously stirred overnight. For the ^{1}H NMR measurement, 4,4-dimethyl-4-silapentane-1-sulfonic acid (DSS; 6.0 μmol) was added to D_2O-rich phase as an internal standard. The symbols "*" indicate signals that arise from the organic solvent.

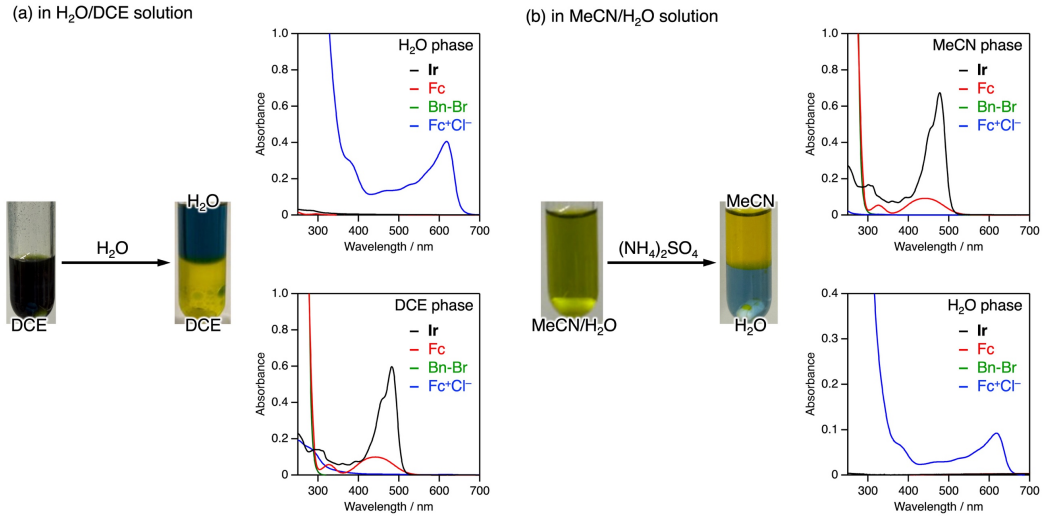

Fig. S4 Photographs and UV-vis absorption spectra of aqueous and DCE or MeCN phases containing **Ir**, Fc, Bn-Br, and Fc^+Cl^- in a (a) H_2O/DCE and (b) MeCN/H_2O in the absence and presence of $(NH_4)_2SO_4$ (2 M for 1 mL H_2O).

Table S2 Partition coefficients of each component[a]

Solution	C_{H2O}/C_{Org}				
	Fc	**Ir**	Bn-Br	Fc^+Cl^-	$TBAHSO_4$ [c]
H_2O/DCE	2×10^{-5}	1×10^{-6}	1×10^{-6}	122	0.11
MeCN/H_2O[b]	5×10^{-6}	1×10^{-6}	1×10^{-6}	54	~0

[a] Estimation based on the absorption spectra of each solution phase of their biphasic solution. [b] In the presence of 2 M $(NH_4)_2SO_4$. [c] Estimation based on the ^1H NMR spectra of D_2O phase (see Fig. S5).

Table S3 Bulk organic-phase properties and biphasic parameters of the solvent systems, along with photochemical Fc^+ formation

Entry	Solution	Organic-phase properties		Biphasic parameters		Generated Fc^+ / μmol[c]
		μ / mPa s[a]	D / 10^{-5} cm^2 s^{-1}	$[(NH_4)_2SO_4]$ / M[b]	Miscibility	
1	H_2O/DCE	0.78	1.0	0	Biphase	1.38
2	DCE	0.78	1.0	–	Single phase	0
3	H_2O/MeCN	0.87[d]	0.8[e]	0	Single phase	0
4	H_2O/MeCN	0.34[f]	2.8[f]	0.5	Biphase	0.13
5	H_2O/MeCN	0.34[f]	2.8[f]	1.0	Biphase	0.17
6	H_2O/MeCN	0.34[f]	2.8[f]	1.5	Biphase	0.22
7	H_2O/MeCN	0.34[f]	2.8[f]	2.0	Biphase	0.30
8	H_2O/DCM	0.41	2.4	0	Biphase	1.69
9	H_2O/DCB	1.32	0.4	0	Biphase	1.17
10	H_2O/DCM	0.41	2.4	2.0	Biphase	1.69
11	H_2O/DCE	0.78	1.0	2.0	Biphase	2.17
12	H_2O/DCB	1.32	0.4	2.0	Biphase	1.47

[a] at 25ºC.[8] [b] Additive to aqueous phase. [c] Standard conditions: Fc (5.0 mM), **Ir** (0.05 mM), and Bn-Br (50 mM) in a H_2O/organic solution (2 mL, 1:1, *v*/*v*) under visible light irradiation (λ = 470 nm, 60 min). For entries 3–7, $TBAHSO_4$ (5.0 mM) was added to the organic phase unless otherwise noted. [d] ref.[9] [e] In mixed solution MeCN/H_2O (1:1, *v*/*v*). [f] In pure MeCN solution.

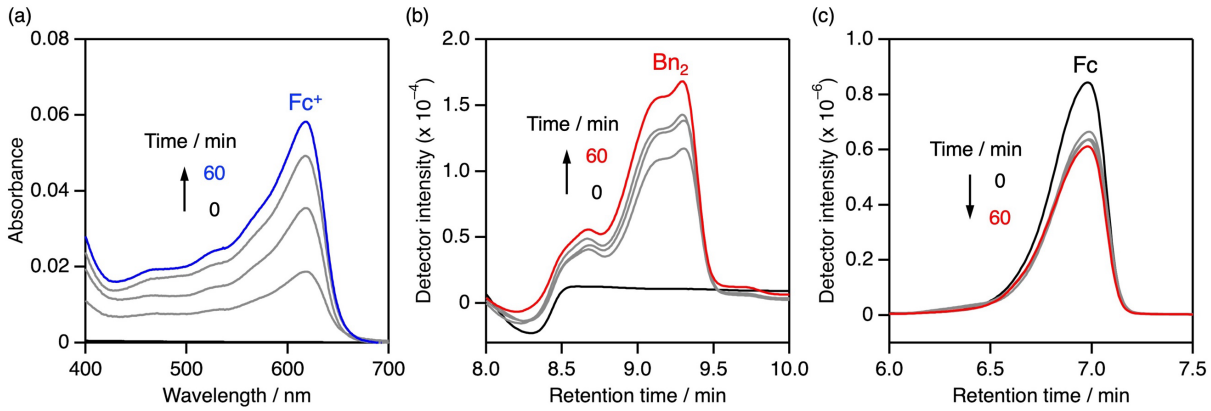

Fig. S5 (a) UV-vis absorption spectra of the aqueous phase for Fc^+ formation, and HPLC chromatograms of the DCE solution phase in the region of (b) Bn_2 formation and (c) Fc consumption.

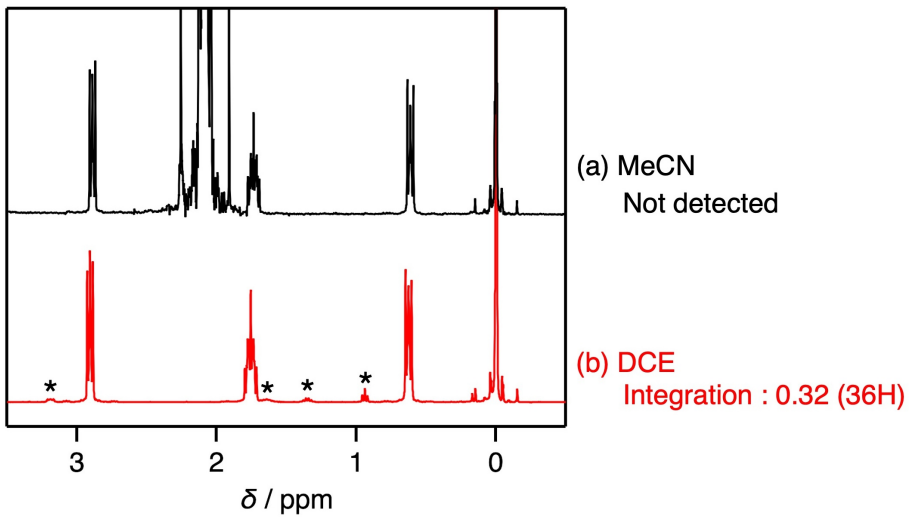

Fig. S6 ^{1}H NMR spectra of D_2O-rich phase for estimating partition coefficients of $TBAHSO_4$: A biphasic solution containing (a) D_2O/DCE and (b) MeCN/D_2O salting-out system (2.0 M $(NH_4)_2SO_4$) (2 mL; 1:1, *v*/*v*) in the presence of $TBAHSO_4$ (1.0 mM) was vigorously stirred 10 min. For the ^{1}H NMR measurement, DSS (6.0 μmol) was added to D_2O-rich phase as an internal standard (see Table S1). The symbols "*" indicate signals that arise from TBA^+. Partition coefficients of $TBAHSO_4$ were estimated as follows: $C_{H2O}/C_{DCE} = 0.11$ and $C_{H2O}/C_{MeCN} \sim 0$.

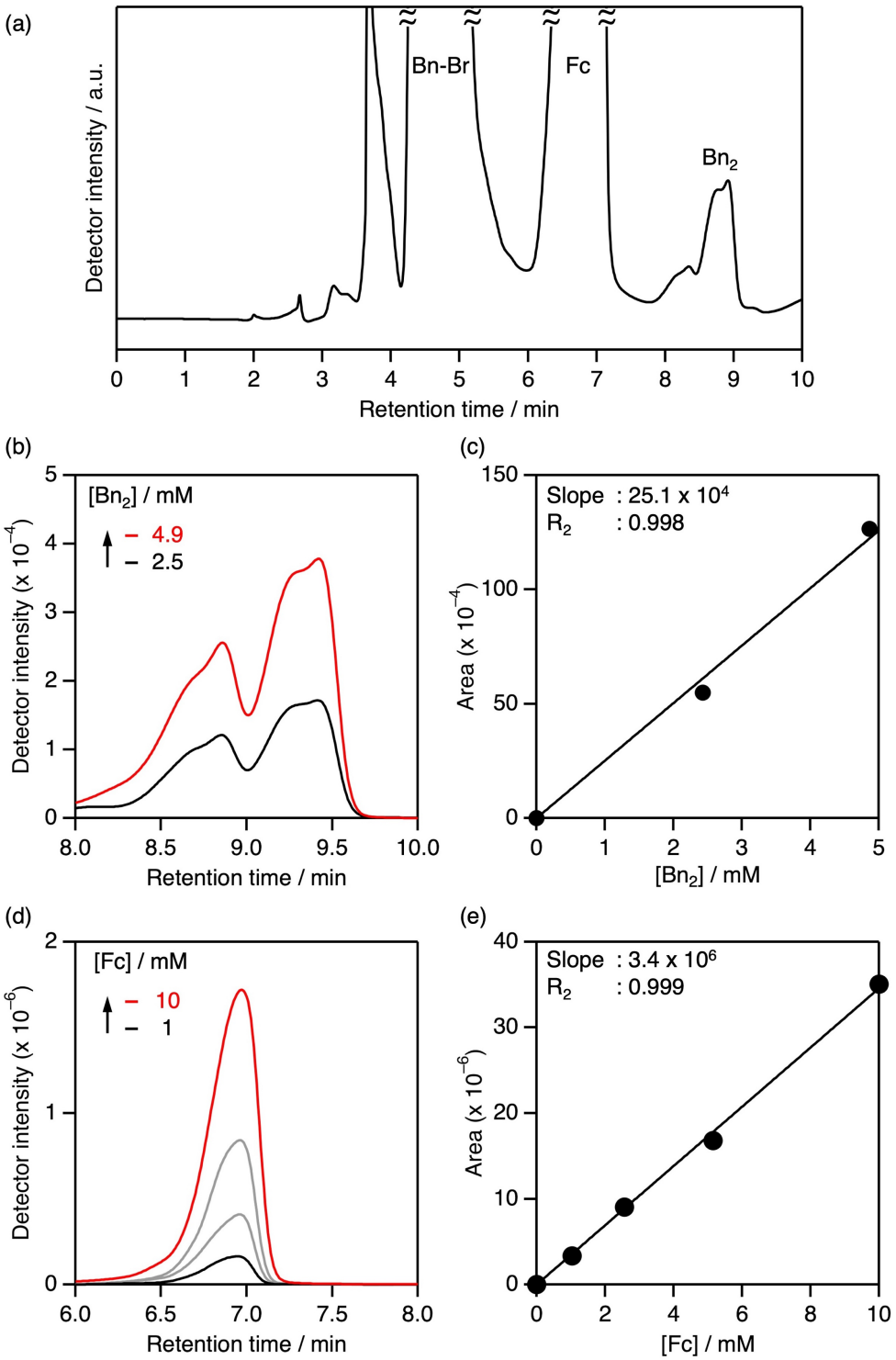

Fig. S7 (a) HPLC chromatograms of DCE solution containing Fc, Bn-Br, and Bn_2, and HPLC chromatograms and calibration curves of DCE solutions containing various concentrations of (b,c) Bn_2 and (d,e) Fc.

References

1. S. Takizawa, N. Ikuta, F. Zeng, S. Komaru, S. Sebata and S. Murata, *Inorg. Chem.*, 2016, **55**, 8723-8735.
2. S. Sebata, S. Takizawa, N. Ikuta and S. Murata, *Dalton Trans.*, 2019, **48**, 14914-14925.
3. R. Breuer and M. Schmittel, *Organometallics*, 2012, **31**, 1870-1878.
4. A. Singh, D. R. Chowdhury and A. Paul, *Analyst*, 2014, **139**, 5747-5754.
5. J. P. Hurvois and C. Moinet, *J. Organomet. Chem.*, 2005, **690**, 1829-1839.
6. G. Zotti, G. Schiavon, S. Zecchin and D. Favretto, *J. Electroanal. Chem.*, 1998, **456**, 217-221.
7. H. Boaz and G. K. Rollefson, *J. Am. Chem. Soc.*, 1950, **72**, 3435-3443.
8. Y. Marcus, *The Properties of Solvents*, Wiley, Chichester, 1998.
9. M. Ansari and S. P. Singh, *Res. J. Chem. Sci.*, 2022, **12**, 67-69.